inorganics

MDPI

Article

Alternative Synthesis of MCM-41 Using Inexpensive Precursors for CO_2 Capture

Guillermo D. Aquino [1,2], M. Sergio Moreno [3], Cristian M. Piqueras [4], Germán P. Benedictto [1,2] and Andrea M. Pereyra [1,5,*]

1 Centro de Investigación y Desarrollo en Ciencias Aplicadas (CINDECA), UNLP-CONICET, La Plata 1900, Argentina; guillermo.aquino.94@gmail.com (G.D.A.); german.benedictto@gmail.com (G.P.B.)
2 Laboratorio de Investigaciones Químicas, FRA, UTN, Villa Domínico 1874, Argentina
3 Instituto de Nanociencia y Nanotecnología (INN), CNEA-CONICET-CAB, San Carlos de Bariloche 8402, Argentina; meketo@gmail.com
4 Planta Piloto de Ingeniería Química (PLAPIQUI), UNS-CONICET, Bahía Blanca 8000, Argentina; cpiqueras@plapiqui.edu.ar
5 Centro de Investigación y Desarrollo en Tecnología de Materiales (CITEMA), FRLP, UTN-CICPBA, La Plata 1900, Argentina
* Correspondence: andreampereyra@yahoo.com

Abstract: We explore the use of industrial sources of silicon and surfactant for obtaining low-cost MCM-41 materials and evaluate their performances as CO_2 adsorbents. All of them presented a high specific surface area with different structural characteristics and textural properties. Interestingly, the MCM-41 manufactured with the most economical reagents presented a S_{BET} of 1602 $m^2 \cdot g^{-1}$. The template was removed by using thermal treatments in an air atmosphere or a washing process. Preservation of silanol groups proved to be more effective under washing or mild thermal treatment conditions with the advantage of their lower cost and environmental benefit. Surface reactivity against CO_2 was enhanced by anchoring APTS to silanol groups through wet grafting. All amino-functionalized materials showed a performance as CO_2 adsorbents comparable to those reported in the literature, reaching values close to 30 $cm^3 \cdot g^{-1}$ at 25 °C and 760 mmHg. Samples with a higher concentration of silanol groups showed better performance. Our studies indicate that adsorbed CO_2 is retained at least up to 50 °C, and the CO_2 is chemisorbed on the silica modified with amine groups. The chemisorbed gas at very low pressures points to the potential use of these materials for CO_2 storage.

Keywords: MCM-41; industrial reactants; silanol group preservation; CO_2 capture

Citation: Aquino, G.D.; Moreno, M.S.; Piqueras, C.M.; Benedictto, G.P.; Pereyra, A.M. Alternative Synthesis of MCM-41 Using Inexpensive Precursors for CO_2 Capture. *Inorganics* **2023**, *11*, 480. https://doi.org/10.3390/inorganics11120480

Academic Editors: Roberto Nisticò, Torben R. Jensen, Luciano Carlos, Hicham Idriss and Eleonora Aneggi

Received: 25 October 2023
Revised: 7 December 2023
Accepted: 11 December 2023
Published: 14 December 2023

1. Introduction

The ongoing challenge of global warming is a pressing environmental issue of significant concern. In response to the need to reduce CO_2 emissions, the development of carbon capture and storage (CCS) technologies has emerged as a promising alternative [1]. CCS includes diverse methodologies such as absorption, adsorption, membrane-based systems, and cryogenic separation [2]. In this context, the application of porous materials as adsorbents is gaining substantial attraction due to its advantages, including low energy requirements for adsorbent regeneration, high adsorption capacity, and selectivity for CO_2.

Numerous adsorbents have been proposed and developed, such as activated carbon [3], zeolites [4], mesoporous silicas [5], lamellar double hydroxides [6], metal–organic frameworks [7], graphene oxide [8], and magnesium oxide-based adsorbents [9]. Among these materials, mesoporous silicas have emerged as particularly noteworthy candidates, due to their well-defined pore structures, high surface areas, and chemical surface compositions, suitable for functionalization with reactive species for CO_2 chemisorption. In particular, amine-modified MCM-41 is effective in capturing CO_2, with reported sorption capacities between 0.87 and 2.41 mmol/g under different adsorption conditions [10–18].

Nowadays, a persistent challenge involves improving the efficiency of existing adsorbents while reducing production costs. Achieving this balance is critical for the widespread use of CO_2 adsorption technologies at an industrial scale. In this regard, considerable attention has been given to template agent removal procedures. Thermal treatments are proven to be both fast and effective in removing surfactants, as reported in most of the current literature that analyses MCM-41 silicas as CO_2 adsorbents [10–13]. However, they also produce the condensation of silanol groups into siloxane bonds when applied at temperatures above 270 °C with a detrimental effect on the functionalization capability of the material [19]. Moreover, the combustion of the organic template also leads to CO_2 emission, which is contrary to the potential application of these adsorbent materials [19]. An alternative consists of the use of washing methodologies for template removal. Conversely, employing solvents may offer the advantage of retaining these essential groups and avoiding CO_2 emissions. On the other hand, inefficient extraction might lead to incomplete template removal, resulting in materials with diminished surface areas and restricted accessibility to the silanol groups. In addition, it is necessary to consider the environmental impact of chemical solvents employed in the washing procedure.

Once the porosity of the MCM-41 silicas has been released, surface modification becomes necessary to enhance their efficacy as carbon dioxide adsorbents. Among the different molecules used for this purpose, amines stand out, given their highly selective CO_2 uptake [20]. The 3-aminopropyltrimethoxysilane (APTS) is broadly used, due to its low cost and relatively small size, for its incorporation into the MCM-41 through two methodologies: dry grafting [10,12,14–16] and wet grafting [11,13]. It has been proven that wet conditions promote materials with higher CO_2 adsorption capacities. This was attributed to the role of water in the generation of silanol groups on the silica surface during the grafting process, which serve as new active sites for the anchoring of 3-aminopropyl groups [17].

In this work, the use of low-cost industrial sources of silicon and surfactants for the synthesis of MCM-41 mesoporous silica was explored. An alkaline silicate solution was used as a source of silicon, and the template consisted of a hydroalcoholic solution of CTAC that is currently used as a wetting agent in the plastic and textile industry. Different methodologies for template removal were applied to maximize surface areas while safeguarding the surface-bound silanol groups, minimizing energy consumption, and using environmentally friendly reagents. The materials were surface modified by grafting with APTS to enhance CO_2 adsorption properties, and their retentions were evaluated as functions of temperature by in situ Fourier transform infrared spectra (FTIR).

2. Experimental Procedure

2.1. Materials

The reactants used in this study were tetraethyl orthosilicate (TEOS 98%, Aldrich, St. Louis, MO, USA), industrial sodium silicate solution (ISS, 27.35 wt% SiO_2 and 8.30 wt% Na_2O, Mejorsil, Quilmes, Argentina), hexadecyltrimethylammonium bromide (CTAB 96%, Sigma-Aldrich, St. Louis, MO, USA), industrial N-hexadecyltrimethylammonium chloride (CTAC, 48–50 wt% CTAC, 30–35 wt% EtOH, and less than 1 wt% N,N-dimethylhexadecylamine (DMHA), Meranol, Avellaneda, Argentina), sulfuric acid (H_2SO_4, 98%, Anedra, Los Troncos del Talar, Argentina), ammonia (25%, Merck, Darmstadt, Germany), absolute ethyl alcohol (99.5%, Soria Analytical, Buenos Aires, Argentina), and 3-aminopropyltrimethoxysilane (97%, Sigma-Aldrich).

2.2. Synthesis and Functionalization

Different sources of silicon and structure-directing agents were explored. The samples were identified considering the silicon source, surfactant, and the thermal treatment used to remove the template.

The MCM-41 synthesized from ISS and CTAB or CTAC industrial solution was obtained following the methodology proposed by Edler [21]. In a typical preparation, CTAB

or CTAC was dissolved in deionized water under stirring at 30 °C until a clear solution was obtained. Then, ISS was added dropwise to the mixture under vigorous stirring. After 15 min under stirring, the pH was adjusted using a solution of H_2SO_4 (10 wt%). The composition of the obtained gel was 1 SiO_2: 0.29 Na_2O: 0.25–0.26 CTAB or CTAC: <0.006 DMHA: 1.09–1.27 EtOH: 155.47–156.12 H_2O. The mixture was then transferred to a Teflon-lined stainless-steel autoclave and kept in an oven at 100 °C for 4 h. After that, the solid was filtered, washed with deionized water, and dried at 100 °C for 24 h. The samples were called S-B and S-C, respectively.

A reference sample was prepared by using TEOS and CTAB [22]. The molar composition was 1 TEOS: 0.3 CTAB: 11 NH_4OH: 58 EtOH: 144 H_2O. The medium synthesis temperature was 30 °C. The complete dissolution of CTAB was ensure, and, subsequently, the silicon source was added dropwise under stirring at 30 °C for 2 h. The material was recovered by filtration and washed with ethanol and then with distilled water. Finally, excess moisture was removed by drying it at 100 °C for 24 h. The sample was called T-B.

The surfactant was removed using different thermal treatments in air: A long treatment (LT, 540 °C for 10 h, heating rate 1 °C/min) or a short treatment (ST, 510 °C for 2 h, 5 °C/min). Samples were called S-B-LT, S-B-ST, S-C-LT, S-C-ST, T-B-LT, and T-B-ST, respectively.

To avoid the condensation of silanol groups induced by thermal treatments [23], a washing process with ethanol (i.e., solvent extraction) under acidic conditions at 70 °C for 40 min was used to remove the template [24]. This procedure was repeated 4 times, mixing the sample previously extracted with a fresh solvent solution. Finally, the solid was dried at 100 °C for 24 h. The samples were identified by the -W suffix.

Once the surfactant was removed, the materials were functionalized with APTS by the grafting method reported in reference [13]. The MCM-41 was added to anhydrous ethanol under stirring for 10 min. Then, distilled water was added under continuous stirring for 30 min. The APTS was added dropwise at 70 °C. The mixture was stirred and refluxed for 10 h. The APTS-modified material was obtained after washing with anhydrous ethanol and drying at 80 °C for 12 h. Samples were called S-B-ST-g, T-B-ST-g, S-C-ST-g, and S-C-W-g.

Figure 1 illustrates the different synthesis routes followed in this work.

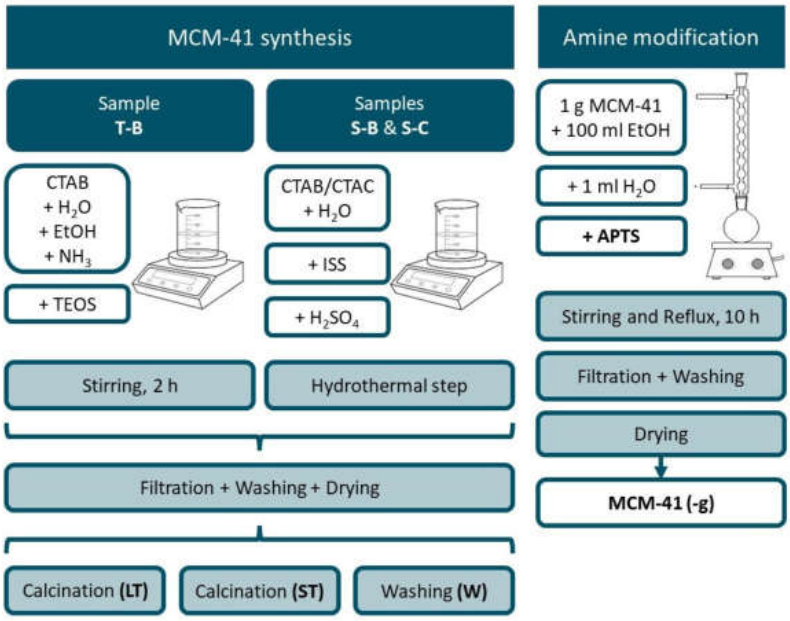

Figure 1. Synthesis and functionalization scheme.

2.3. Characterization

The small angle X-ray diffraction patterns (SAXS) were obtained using XENOCS (Santa Barbara, CA, USA) XEUSS 1.0 equipment with a Pilatus 100K detector with Cu Kα

radiation (λ = 1.5405 Å). Scanning electron microscopy (SEM) images were acquired on an FEI (Hillsboro, OH, USA) Inspect S50 microscope operated at 2 kV. The samples were sputtered with a thin film of gold. Transmission electron microscopy (TEM) was performed using a FEI (Hillsboro, OH, USA) Tecnai F20 G2 microscope operated at 200 kV. FTIR spectra were obtained in a Thermo Fisher Scientific (Buenos Aires, Argentina) FTIR Nicolet iS5 spectrophotometer with an iD5 ATR accessory.

The N_2 adsorption–desorption isotherms at 77 K were measured on Micromeritics (Buenos Aires, Argentina) ASAP 2020 apparatus. Prior to the analysis, the samples were degassed at 100 °C for 12 h under a vacuum of 10^{-2} mmHg. The specific surface area was obtained from the gas adsorption isotherms by applying the Brunauer–Emmett–Teller theory (S_{BET}) and non-local density functional theory (S_{DFT}). The total pore volume (V_P) was estimated using the Gurvich rule at a relative pressure of 0.953 [25]. The pore size distribution (PSD) analysis was performed using the NLDFT model applied to cylindrical pores and an oxide surface.

2.4. CO_2 Adsorption Testing

The CO_2 adsorption/desorption isotherms were measured in Quantachrome (Boynton Beach, USA) Autosorb iQ model automatic sorption equipment with its control and data analysis software (ASiQwin 6.0). The samples were introduced into a 12 mm diameter quartz cell provided for the chemisorption mode. The isotherms were fitted using the Langmuir isotherm to determine the moles of CO_2 sorbed in a monolayer covering the surface. CO_2 isotherms were obtained at 25 °C in the pressure range from 10 to 800 Torr.

Diffuse reflectance infrared spectroscopy (DRIFTS) measurements were performed on a Thermo Fisher Scientific (Buenos Aires, Argentina) Nicolet 6700 with a low-temperature high sensitivity Thermo Fischer MCT-A detector. This equipment was assembled with a sealed cell that allowed the treatment of samples with gases at a controlled temperature. Spectra were taken after dosing 5 Torr of CO_2 and then in vacuum at different temperatures up to 100 °C.

3. Results and Discussion

The SAXS diffraction patterns shown in Figure 2 are consistent with the expected 2D hexagonal structure (plane group p6m) and are indexed accordingly. The samples synthesized with ISS exhibited a higher degree of order. Among them, the one obtained using CTAC presented broadened reflections. It can be observed that a longer thermal treatment at higher temperature (LT) produced a slight decrease in the interpore distance from 4.64 to 4.57 nm for the S samples and from 4.02 to 3.83 nm for the T samples. The number of observed reflections indicated high-quality samples in the bulk analysis, confirming a well-ordered hexagonal structure.

The SEM images (Figure 3) showed morphological differences depending on the silicon source. Samples made using TEOS had a spherical shape, whereas those synthesized with sodium silicate presented a more irregular geometry and a smaller particle size.

In Figure 4, representative TEM images of each sample are shown. Different morphologies are observed. Samples obtained using ISS tend to present porous structures organized at different spatial scales. S-C samples presented particles with a bowl shape and shorter mesochannels compared to samples S-B. Mesochannels in S-C materials are oriented more randomly than those in S-B samples due to their lengths. Samples T-B have a spherical shape with a broad particle size distribution and radial mesochannels.

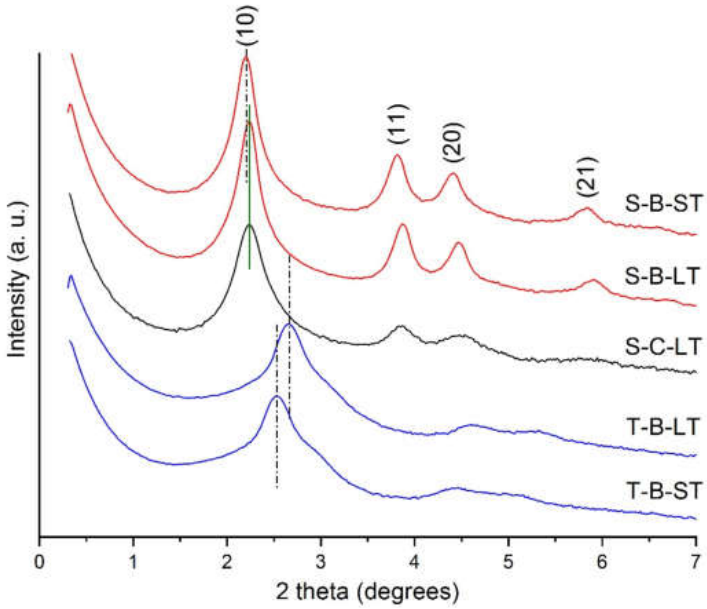

Figure 2. SAXS of MCM-41 samples.

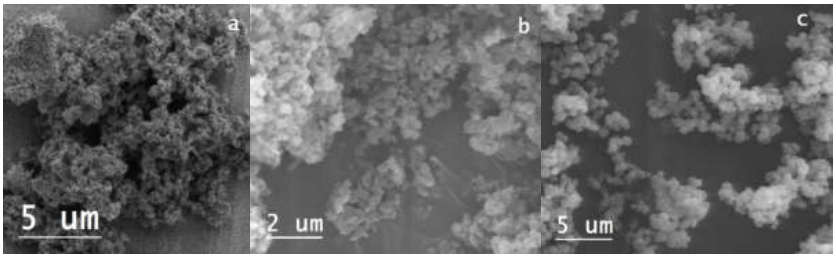

Figure 3. SEM images of samples S-C (**a**), S-B (**b**), and T-B (**c**).

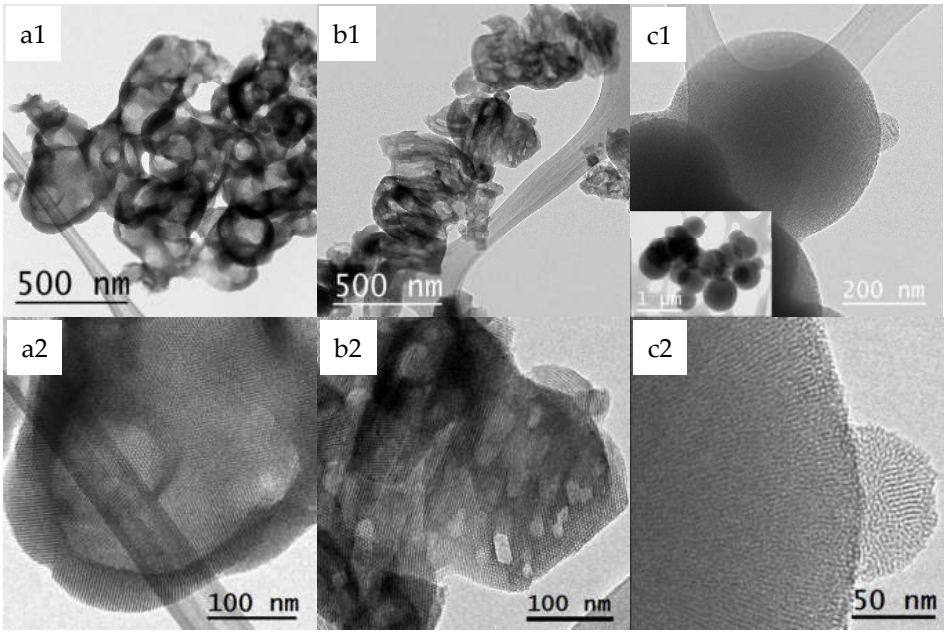

Figure 4. TEM images at different magnifications of samples S-C-ST (**a1**,**a2**), S-B-ST (**b1**,**b2**), and T-B-ST (**c1**,**c2**).

Before textural analysis, the surfactant elimination was verified by FTIR. Spectra of the S-C sample before and after removal treatments are shown in Figure 5 (left). Similar results were obtained for S-B and T-B samples.

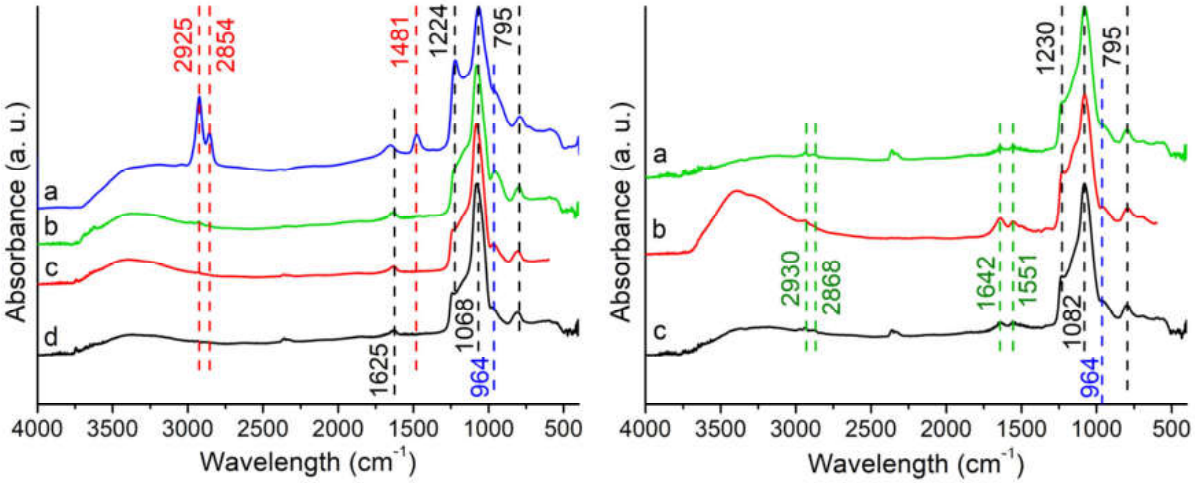

Figure 5. FTIR spectra of S-C samples: (**Left**) (a) as-made, (b) S-C-W, (c) S-C-ST, and (d) S-C-LT; (**Right**) (a) S-C-W-g, (b) S-C-ST-g, and (c) S-C-LT-g. Bands attributed to surfactant (red lines), silanol groups (blue line), aminopropyl groups (green lines), and Si-O modes (black lines) are indicated.

The spectra of as-made samples showed bands attributed to the surfactant at 2854 cm^{-1}, 2925 cm^{-1}, and 1480 cm^{-1} [26,27]. These bands are assigned to C-H asymmetric stretching of alkyl chains of CTA cation and symmetric and asymmetric stretching C-H scissoring vibration of the CH_3-N^+ group. The absence of these bands after treatments indicated the removal of the template. Other bands observed between 1224 cm^{-1} and 795 cm^{-1} are assigned to different Si-O modes [28,29]. The preservation of silanol groups was confirmed by the band at 964 cm^{-1} (blue line), which corresponds to the stretching vibrations of the surface Si-O- groups [28,30–32]. Bands observed at 1625 cm^{-1} and 3400 cm^{-1} are assigned to OH bending vibrations and -OH units of adsorbed water and silanol groups [28].

From the point of view of preservation of silanol groups, solvent extraction and ST treatment seem to be more efficient than the longer one. The incorporation of APTS molecules was confirmed (Figure 5, right) by the appearance of the bands at 2925 cm^{-1} and 2854 cm^{-1} (C-H bonds) and 1642 cm^{-1} (N-H deformation in RNH_3^+) [33].

An indication of the high reactivity of the functionalized material against CO_2 adsorption was evidenced by the presence of the band around 1555 cm^{-1} (C=O stretch), which is attributed to carbamate formed by the exposure to air [33–35]. The symmetric and asymmetric stretching modes of CO_2^- could be seen around 2349 cm^{-1}, 1386 cm^{-1}, and 1430 cm^{-1} [20,36].

Nitrogen adsorption and desorption isotherms and the PSD for the synthesized materials subjected to ST treatment and for their functionalized counterparts are shown in Figure 6. The main textural parameters obtained from different methods are compiled in Table 1, with the sample S-C-ST showing the best textural properties.

Nitrogen isotherms from S-C-ST and S-B-ST can be classified as type IV according to the IUPAC classification, which is characteristic of mesoporous materials. When examining the curves, two different hysteresis loops can be seen. The first one corresponds to H1 type and appears at a relative pressure of around 0.35. This can be attributed to a narrow pore size distribution of the open-ended tubular pores from MCM-41 material framework [25]. The second one extends over the relative pressure range of 0.46–0.95. This hysteresis loop can be associated with the existence of the porosity observed at a bigger scale, as revealed in the TEM images. On the other hand, T-B-ST exhibits a type I-like isotherm, as reported elsewhere [37,38]. Samples S-C-ST and S-B-ST presented a narrow PSD with a pore diameter of about 4 nm.

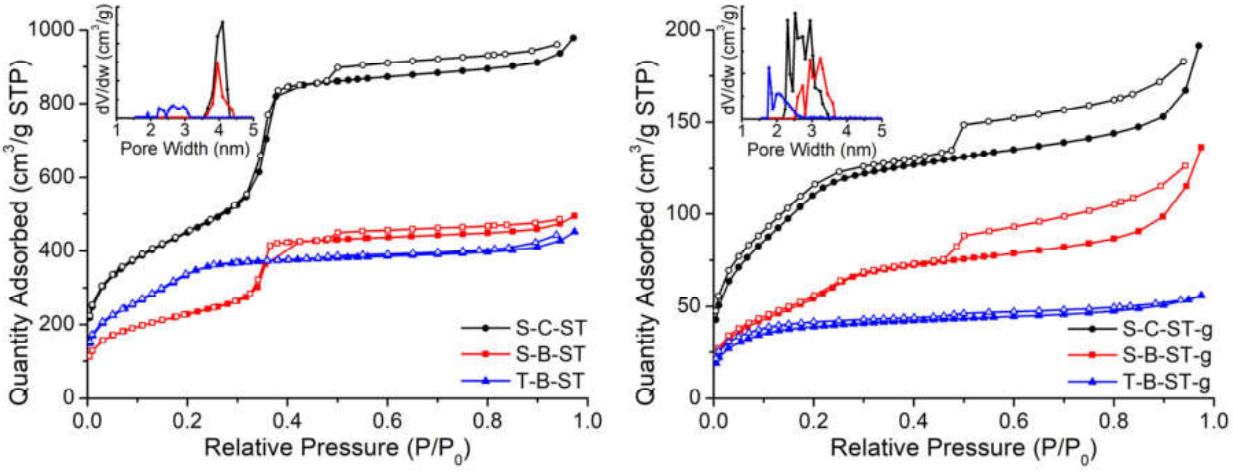

Figure 6. N_2 adsorption (solid symbols) and desorption (open symbols) isotherms of as-made (**left**) and amine-modified (**right**) MCM-41.

Table 1. Textural parameters for MCM-41 materials obtained from N_2 adsorption isotherms.

Sample	S_{BET} (m^2/g)	S_{DFT} (m^2/g)	V_P (cm^3/g)	$D_{P\ NLDFT}$ (nm)
S-C-W	760	608	0.68	3.95
S-C-LT	992	818	0.86	3.95
S-C-ST	1602	1356	1.45	4.10
S-C-ST-g	398	295	0.26	2.24–3.45
S-B-ST	812	673	0.73	3.95
S-B-ST-g	196	152	0.18	2.50–3.60
T-B-ST	1200	886	0.66	2.24–3.10
T-B-ST-g	138	121	0.083	1.77–2.67

After amine modification, the textural parameters decreased significantly. Samples synthesized using ISS (S-C-ST g and S-B-ST-g) presented isotherms similar to type I, preserving the H4 hysteresis loop. This might suggest a reduction in the MCM-41 channel diameter. The second loop seems to be preserved. However, T-B-ST-f exhibited a full type I isotherm commonly attributed to microporous materials, after amine modification, which agrees with the shift of PSD to lower values. In addition, amine-modified samples did not display fully reversible isotherms over the complete relative pressure range. A similar behavior occurs in activated carbons with the only presence of micropores, where the solid wall potential has a great influence on physical adsorption [39].

Estimating the surface area of adsorbents with mesopores in the range of 20 to 40 Å, such as MCM-41 and MCM-48, using the BET approach can pose challenges. In this case, pore filling takes place at pressures very near the range where the formation of monolayer-multilayer structures on the pore walls occurs. This phenomenon is a consequence of the growing potential of pore walls during the condensation process [40]. The presence of these multilayer structures leads to a significant overestimation of the monolayer capacity when conducting BET analysis. As a response to this challenge, we chose to present the surface area reported by the NLDFT model. These models account for the increasing potential of the walls concerning nitrogen adsorption as pore size decreases, thereby yielding more dependable and accurate surface area results.

3.1. CO_2 Adsorption Performance

The CO_2 sorption isotherms are shown in Figure 7. In the upper left panel, the results for different sources of silicon and surfactant for ST samples are compared. The isotherms are similar to those of type I of the IUPAC classification [41], in which the sorption of CO_2 on the surface can be described without the formation of a multilayer

for the pressure range up to 800 mmHg. They can be fitted by the Langmuir isotherm, indicating monolayer adsorption. The physisorption isotherms are nearly identical to the sorption ones, suggesting that the adsorption is almost completely of a physical nature. However, all samples exhibited nonreversible isotherms, which might indicate some degree of CO_2 chemisorption. The samples functionalized significantly increased the sorption of CO_2 [42]. The adsorbed volumes are comparable to those found in the literature (see Table 2). All modified samples exhibited similar adsorption curves, with S-C-ST g material demonstrating a slightly better performance at higher pressures. This might be due to its superior textural properties.

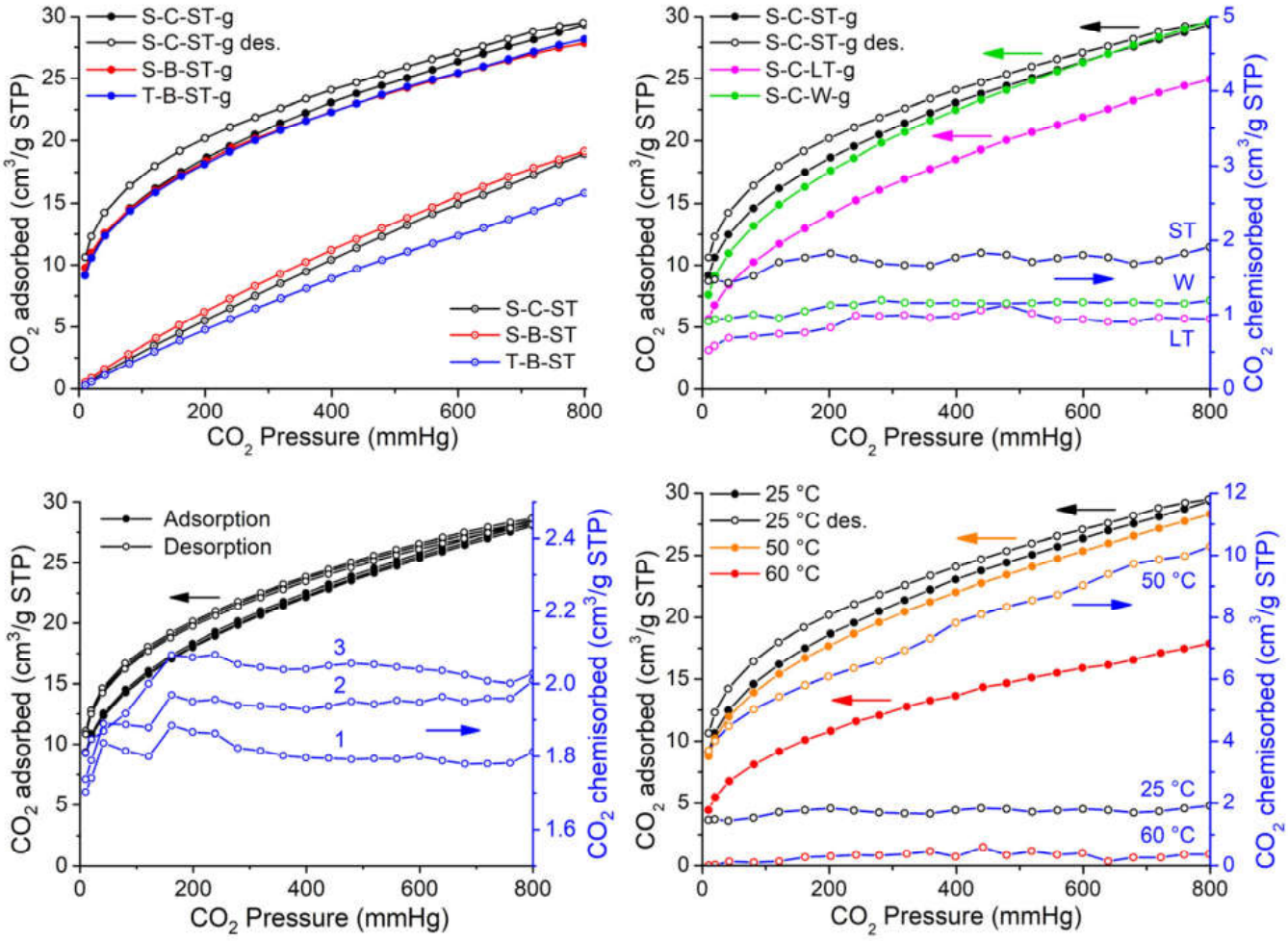

Figure 7. CO_2 total sorption isotherms at 25 °C of as-made and amine-modified MCM-41 (**upper panels**). Sorption isotherms of three consecutive cycles and adsorption/desorption isotherms at different temperatures for S-C-ST g sample (**lower panels**).

Table 2 summarizes the results for our materials and similar ones reported in the literature. When available, it can be seen that there is a great variation in the conditions of the studies and the preparation of reported samples. Our studies presented a slightly better performance than those carried out at similar conditions of pressure and temperature [10,12,14,15]. Other studies performed under dynamic conditions led to higher adsorption values [11,13]. In all cases, textural properties decreased after amine modification.

Table 2. CO_2 adsorption for amine-modified samples and results available in the literature.

Material			Amine-Modified Material		CO_2 Adsorption			Reference
	Si Source	S_{BET} (m^2/g)/V_P (cm^3/g)	Modification	S_{BET} (m^2/g)/V_P (cm^3/g)	Temp. (°C)	CO_2 Pressure (mmHg)	CO_2 Adsorbed (mmol/g)	
MCM-41	ISS	760/0.68	APTS, WG	--/--	25	760	1.29	S-C-W-g
MCM-41	ISS	992/0.86	APTS, WG	--/--	25	760	1.09	S-C-LT-g
MCM-41	ISS	1602/1.45	APTS, WG	398/0.26	25	760	1.28	S-C-ST-g
MCM-41	ISS	812/0.73	APTS, WG	196/0.18	25	760	1.22	S-B-ST-g
MCM-41	TEOS	1200/0.66	APTS, WG	138/0.08	25	760	1.24	T-B-ST-g
MCM-41	--	997/0.90	APTS, WG	958/0.51	70	114	1.88	[13]
MCM-41	TEOS	1059/0.68	APTS, DG	198/0.13	Room temp.	750	1.15	[10]
SBA-15	TEOS	548/0.95	APTS, DG	304/0.55		750	0.93	
MCM-41	TEOS	894/1.28	APTS, DG	544/0.74	45	750	0.87	[14]
MCM-41	TEOS	992/0.69	APTS, WG	736/0.37	25	750	2.41	[11]
MCM-41	--	1031/0.90	APTS, DG	17/0.04	20	750	1.07	[12]
					30	750	0.96	
MCM-41	TEOS	1045/2.59	APTS, DG	--/--	30	750	1.20	[15]
MCM-41	Sodium silicate Merck	864/0.62	APTS, DG	207/0.13	30	3.8	0.39	[16]
SBA-15	TEOS	782/0.73	APTS, DG	280/0.29	60	114	1.06	[17]
SBA-15	TEOS	766/1.32	TRI-s, DG	177/0.49	25	760	1.30	
			TRI-s, WG	112/0.31			1.66	
Bimodal silica	TEOS	612/1.59	TRI-s, DG	203/0.96			1.73	
			TRI-s, WG	71/0.56			1.96	
Hierarchically Ordered Porous Silica	TEOS	1045/0.58	APTS, DG	781/0.45	0	750	1.98	[18]

APTS: aminopropyltrimethoxysilane or aminopropyltriethoxysilane; TRI-s: N1-(3-Trimethoxysilylpropyl)diethylenetriamine; WG: Wet grafting; DG: Dry grafting; '--': No data available.

In the upper right panel, the effects of the method used to remove the surfactant on the CO_2 sorption isotherms are compared. The long treatment has a deleterious effect on the CO_2 adsorption performance. This might be attributed to a diminished concentration of silanol groups on the surface. Interestingly, the S-C-W g sample has a very similar performance to the S-C-ST-g, with considerable economic and environmental benefits. The better performance of -ST and -W samples can be rationalized based on the stronger Si-OH signal observed in FTIR and the employed wet grafting methodology, which induced the formation of new silanol groups helping to create new active sites for aminopropyl anchoring [17].

Figure 7 (left lower panel) shows the sorption isotherms of three consecutive cycles for the S-C-ST g sample. The adsorption and desorption are comparable. A progressive small difference in chemisorption with cycles is observed, which would reflect a greater number of adsorption sites. This result may be attributed to the progressive removal of surface residue from the surface occupied by active sites for adsorption, added to the fact that the binding of the amine responsible for this chemical adsorption is strongly anchored to the surface of the MCM-41, which is consistent with the existing literature [43].

Upon exposing the sample S-C-ST g to adsorption at different temperatures (Figure 7, right lower panel), it is observed that the combined adsorption decreases slightly between 25 and 50 °C, whereas the chemisorption increases fivefold. As the adsorption temperature is raised to 60 °C, the combined adsorption decreases remarkably, and chemical adsorption is reduced almost to zero. The adsorption energy decreases with increasing temperature; however, it appears that there is a competition between this physical phenomenon and the phenomenon of chemical adsorption, the latter being favored in the range of 25–50 °C.

3.2. FTIR with In Situ CO_2 Adsorption

FTIR measurements were carried out to assess CO_2 retention at different temperatures, Figure 8. The amine-modified samples (S-C-ST-g, S-B-ST-g, and T-B-ST-g) were exposed to a controlled atmosphere of CO_2 (Figure 8 left), and then the spectra were acquired under vacuum at different temperatures. The spectra corresponding to 50 °C and 100 °C are shown in Figure 8 (right).

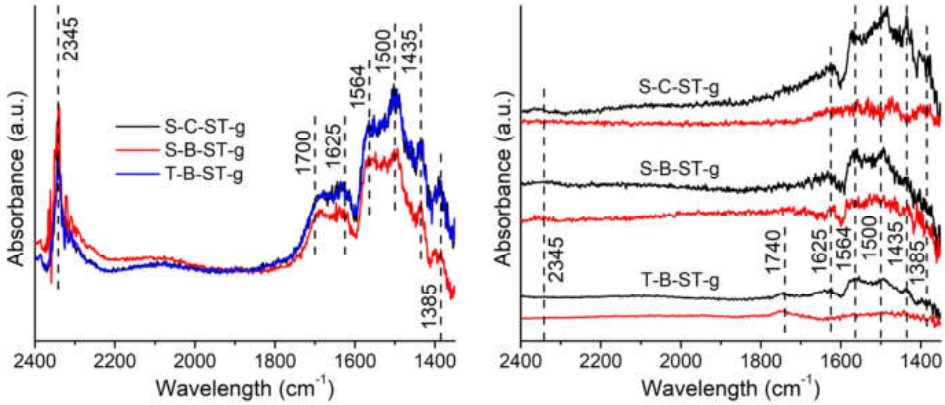

Figure 8. (**Left**) FTIR spectra at 5 Torr of CO_2; (**Right**) Spectra acquired at 50 °C (black) and 100 °C (red).

In all cases, the band attributed to the CO_2 gas phase at 2345 cm^{-1} [36] is observed under the 5 Torr of CO_2 atmosphere. Additional bands are visible in the range 1700–1400 cm^{-1} [20,34,35,44], which could be assigned to the species formed from CO_2 chemisorption on -NH_2 groups. Bands at 1500 cm^{-1} and 1625 cm^{-1} are associated with -NH_3^+ deformation [35]. In the as-made samples, we did not observe bands in this range. It can be concluded that there is no CO_2 chemisorption on the MCM-41 surface without aminopropyl groups. It is corroborated that CO_2 is retained at least up to 50 °C, in agreement with adsorption measurements.

In summary, the response of the functionalized materials shows sensitivity to CO_2 adsorption at very low pressures. This adsorption is retained after high vacuum evacuation at 25 °C. Furthermore, upon heating the sample to 100 °C, the bands corresponding to chemisorbed CO_2 disappear.

4. Conclusions

In this work, inexpensive MCM-41 materials were synthesized successfully using different sources of silicon and surfactants of industrial origin. Surface reactivity was preserved by using gentle methods of template removal, which are environmentally sustainable and implies reducing costs. All of them presented a high specific surface area, but the structural features depended on the reactant nature. Amine-modified materials presented a CO_2 adsorbent capacity comparable with other systems previously reported. The retention of chemisorbed gas at least up to 50 °C at very low pressures suggests the potential of these materials for CO_2 storage. These results combined whit the simplicity of fabrication of the porous materials for the CO_2 sorption constitute a low-cost alternative.

Author Contributions: Conceptualization, G.D.A., A.M.P., G.P.B. and M.S.M.; methodology, G.D.A., A.M.P., G.P.B. and M.S.M.; investigation, G.D.A., A.M.P., G.P.B., C.M.P. and M.S.M.; writing—original draft preparation, G.D.A., A.M.P., G.P.B., C.M.P. and M.S.M.; writing—review and editing, G.D.A., A.M.P., G.P.B., C.M.P. and M.S.M.; project administration, A.M.P. and M.S.M.; funding acquisition, A.M.P. and M.S.M. All authors have read and agreed to the published version of the manuscript.

Funding: This work was financially supported by the Agencia Nacional de Promoción Científica y Tecnológica (ANPCyT) (PICT 2020-03966), Universidad Tecnológica Nacional (PID 8621TC), and Consejo Nacional de Investigaciones Científicas y Técnicas (CONICET) (PIP 11220200100768CO).

Data Availability Statement: The data presented in this study are available in article.

Acknowledgments: The authors thank Paula Troyón for SEM image acquisition.

Conflicts of Interest: The authors declare no conflict of interest.

References

1. Shu, D.Y.; Deutz, S.; Winter, B.A.; Baumgärtner, N.; Leenders, L.; Bardow, A. The Role of Carbon Capture and Storage to Achieve Net-Zero Energy Systems: Trade-Offs between Economics and the Environment. *Renew. Sustain. Energy Rev.* **2023**, *178*, 113246. [CrossRef]
2. Tan, Y.; Nookuea, W.; Li, H.; Thorin, E.; Yan, J. Property Impacts on Carbon Capture and Storage (CCS) Processes: A Review. *Energy Convers. Manag.* **2016**, *118*, 204–222. [CrossRef]
3. Vorokhta, M.; Nováková, J.; Dopita, M.; Khalakhan, I.; Kopecký, V.; Švábová, M. Activated Three-Dimensionally Ordered Micromesoporous Carbons for CO_2 Capture. *Mater. Today Sustain.* **2023**, *24*, 100509. [CrossRef]
4. Cavallo, M.; Dosa, M.; Porcaro, N.G.; Bonino, F.; Piumetti, M.; Crocella, V. Shaped Natural and Synthetic Zeolites for CO_2 Capture in a Wide Temperature Range. *J. CO2 Util.* **2023**, *67*, 102335. [CrossRef]
5. Medina-Juárez, O.; Rangel-Vázquez, I.; Ojeda-López, R.; García-Sánchez, M.Á.; Rojas-González, F. Importance of the Polarity on Nanostructured Silica Materials to Optimize the Hydrolytic Condensation with Molecules Related to CO_2 Adsorption. *Environ. Sci. Pollut. Res.* **2022**, *29*, 58472–58483. [CrossRef]
6. Rocha, C.; Soria, M.A.; Madeira, L.M. Doping of Hydrotalcite-Based Sorbents with Different Interlayer Anions for CO_2 Capture. *Sep. Purif. Technol.* **2020**, *235*, 116140. [CrossRef]
7. Elsabawy, K.M.; Fallatah, A.M. Synthesis of Newly Wings like Structure Non-Crystalline Ni++-1,3,5-Tribenzyl-1,3,5-Triazine-2,4,6-(1H,3H,5H)-Trione Coordinated MOFs for CO_2-Capture. *J. Mol. Struct.* **2019**, *1177*, 255–259. [CrossRef]
8. Shen, Z.; Song, Y.; Yin, C.; Luo, X.; Wang, Y.; Li, X. Construction of Hierarchically Porous 3D Graphene-like Carbon Material by B, N Co-Doping for Enhanced CO_2 Capture. *Microporous Mesoporous Mater.* **2021**, *322*, 111158. [CrossRef]
9. Alkadhem, A.M.; Elgzoly, M.A.A.; Onaizi, S.A. Novel Amine-Functionalized Magnesium Oxide Adsorbents for CO_2 Capture at Ambient Conditions. *J. Environ. Chem. Eng.* **2020**, *8*, 103968. [CrossRef]
10. Zhao, H.; Hu, J.; Wang, J.; Zhou, L.; Liu, H. CO_2 Capture by the Amine-Modified Mesoporous Materials. *Acta Phys.-Chim. Sin.* **2007**, *23*, 801–806. [CrossRef]
11. Rao, N.; Wang, M.; Shang, Z.; Hou, Y.; Fan, G.; Li, J. CO_2 Adsorption by Amine-Functionalized MCM-41: A Comparison between Impregnation and Grafting Modification Methods. *Energy Fuels* **2018**, *32*, 670–677. [CrossRef]
12. Mello, M.R.; Phanon, D.; Silveira, G.Q.; Llewellyn, P.L.; Ronconi, C.M. Amine-Modified MCM-41 Mesoporous Silica for Carbon Dioxide Capture. *Microporous Mesoporous Mater.* **2011**, *143*, 174–179. [CrossRef]
13. Wang, X.; Chen, L.; Guo, Q. Development of Hybrid Amine-Functionalized MCM-41 Sorbents for CO_2 Capture. *Chem. Eng. J.* **2015**, *260*, 573–581. [CrossRef]
14. Sanz, R.; Calleja, G.; Arencibia, A.; Sanz-Pérez, E.S. CO_2 Capture with Pore-Expanded MCM-41 Silica Modified with Amino Groups by Double Functionalization. *Microporous Mesoporous Mater.* **2015**, *209*, 165–171. [CrossRef]
15. Loganathan, S.; Tikmani, M.; Ghoshal, A.K. Novel Pore-Expanded MCM-41 for CO_2 Capture: Synthesis and Characterization. *Langmuir* **2013**, *29*, 3491–3499. [CrossRef] [PubMed]
16. Chang, F.Y.; Chao, K.J.; Cheng, H.H.; Tan, C.S. Adsorption of CO_2 onto Amine-Grafted Mesoporous Silicas. *Sep. Purif. Technol.* **2009**, *70*, 87–95. [CrossRef]
17. Anyanwu, J.T.; Wang, Y.; Yang, R.T. CO_2 Capture (Including Direct Air Capture) and Natural Gas Desulfurization of Amine-Grafted Hierarchical Bimodal Silica. *Chem. Eng. J.* **2022**, *427*, 131561. [CrossRef]
18. Jin, X.; Ge, J.; Zhang, L.; Wu, Z.; Zhu, L.; Xiong, M. Synthesis of Hierarchically Ordered Porous Silica Materials for CO_2 Capture: The Role of Pore Structure and Functionalized Amine. *Inorganics* **2022**, *10*, 87. [CrossRef]
19. Ghaedi, H.; Zhao, M. Review on Template Removal Techniques for Synthesis of Mesoporous Silica Materials. *Energy Fuels* **2022**, *36*, 2424–2446. [CrossRef]
20. Bacsik, Z.; Atluri, R.; Garcia-Bennett, A.E.; Hedin, N. Temperature-Induced Uptake of CO_2 and Formation of Carbamates in Mesocaged Silica Modified with n-Propylamines. *Langmuir* **2010**, *26*, 10013–10024. [CrossRef]
21. Edler, K.J.; White, J.W. Further Improvements in the Long-Range Order of MCM-41 Materials. *Chem. Mater.* **1997**, *9*, 1226–1233. [CrossRef]
22. Grün, M.; Unger, K.K.; Matsumoto, A.; Tsutsumi, K. Novel Pathways for the Preparation of Mesoporous MCM-41 Materials: Control of Porosity and Morphology. *Microporous Mesoporous Mater.* **1999**, *27*, 207–216. [CrossRef]
23. Araujo, A.S.; Jaroniec, M. Thermogravimetric Monitoring of the MCM-41 Synthesis. *Thermochim. Acta* **2000**, *363*, 175–180. [CrossRef]
24. Marcilla, A.; Beltran, M.; Gómez-Siurana, A.; Martinez, I.; Berenguer, D. Template Removal in MCM-41 Type Materials by Solvent Extraction: Influence of the Treatment on the Textural Properties of the Material and the Effect on Its Behaviour as Catalyst for Reducing Tobacco Smoking Toxicity. *Chem. Eng. Res. Des.* **2011**, *89*, 2330–2343. [CrossRef]
25. Rouquerol, J.; Rouquerol, F.; Llewellyn, P.; Maurin, G.; Sing, K.S.W. *Adsorption by Powders and Porous Solids: Principles, Methodology and Applications*, 2nd ed.; Academic Press: Cambridge, MA, USA, 2014; ISBN 9780080970356.

26. Su, G.; Yang, C.; Zhu, J.J. Fabrication of Gold Nanorods with Tunable Longitudinal Surface Plasmon Resonance Peaks by Reductive Dopamine. *Langmuir* **2015**, *31*, 817–823. [CrossRef] [PubMed]
27. Banjare, R.K.; Banjare, M.K.; Panda, S. Effect of Acetonitrile on the Colloidal Behavior of Conventional Cationic Surfactants: A Combined Conductivity, Surface Tension, Fluorescence and FTIR Study. *J. Solut. Chem.* **2020**, *49*, 34–51. [CrossRef]
28. Huo, C.; Ouyang, J.; Yang, H. CuO Nanoparticles Encapsulated inside Al-MCM-41 Mesoporous Materials via Direct Synthetic Route. *Sci. Rep.* **2014**, *4*, 3682. [CrossRef]
29. La-Salvia, N.; Lovón-Quintana, J.J.; Lovón, A.S.P.; Valença, G.P. Influence of Aluminum Addition in the Framework of MCM-41 Mesoporous Molecular Sieve Synthesized by Non-Hydrothermal Method in an Alkali-Free System. *Mater. Res.* **2017**, *20*, 1461–1469. [CrossRef]
30. Li, L.L.; Sun, H.; Fang, C.J.; Xu, J.; Jin, J.Y.; Yan, C.H. Optical Sensors Based on Functionalized Mesoporous Silica SBA-15 for the Detection of Multianalytes (H^+ and Cu^{2+}) in Water. *J. Mater. Chem.* **2007**, *17*, 4492–4498. [CrossRef]
31. Ganji, S.; Mutyala, S.; Neeli, C.K.P.; Rao, K.S.R.; Burri, D.R. Selective Hydrogenation of the CC Bond of α,β-Unsaturated Carbonyl Compounds over PdNPs–SBA-15 in a Water Medium. *RSC Adv.* **2013**, *3*, 11533–11538. [CrossRef]
32. Medeiros de Paula, G.; do Nascimento Rocha de Paula, L.; Freire Rodrigues, M.G. Production of MCM-41 and SBA-15 Hybrid Silicas from Industrial Waste. *Silicon* **2022**, *14*, 439–447. [CrossRef]
33. Qi, G.; Wang, Y.; Estevez, L.; Duan, X.; Anako, N.; Park, A.H.A.; Li, W.; Jones, C.W.; Giannelis, E.P. High Efficiency Nanocomposite Sorbents for CO_2 Capture Based on Amine-Functionalized Mesoporous Capsules. *Energy Environ. Sci.* **2011**, *4*, 444–452. [CrossRef]
34. Knöfel, C.; Martin, C.; Hornebecq, V.; Llewellyn, P.L. Study of Carbon Dioxide Adsorption on Mesoporous Aminopropylsilane-Functionalized Silica and Titania Combining Microcalorimetry and in Situ Infrared Spectroscopy. *J. Phys. Chem. C* **2009**, *113*, 21726–21734. [CrossRef]
35. Socrates, G. *Infrared and Raman Characteristic Group Frequencies: Tables and Charts*, 3rd ed.; John Wiley & Sons, Ltd: Chichester, UK, 2004; ISBN 978-0-470-09307-8.
36. Danon, A.; Stair, P.C.; Weitz, E. FTIR Study of CO_2 Adsorption on Amine-Grafted SBA-15: Elucidation of Adsorbed Species. *J. Phys. Chem. C* **2011**, *115*, 11540–11549. [CrossRef]
37. Schmidt, R.; Stöcker, M.; Hansen, E.; Akporiaye, D.; Ellestad, O.H. MCM-41: A Model System for Adsorption Studies on Mesoporous Materials. *Microporous Mater.* **1995**, *3*, 443–448. [CrossRef]
38. Wloch, J.; Rozwadowski, M.; Lezanska, M.; Erdmann, K. Analysis of the Pore Structure of the MCM-41 Materials. *Appl. Surf. Sci.* **2002**, *191*, 368–374. [CrossRef]
39. Lowell, S.; Shields, J.E.; Thomas, M.A.; Thommes, M. *Characterization of Porous Solids and Powders: Surface Area, Pore Size and Density*; Particle Technology Series; Springer: Dordrecht, The Netherlands, 2004; Volume 16, ISBN 978-90-481-6633-6.
40. Kruk, M.; Jaroniec, M.; Sayari, A. Adsorption Study of Surface and Structural Properties of MCM-41 Materials of Different Pore Sizes. *J. Phys. Chem. B* **1997**, *101*, 583–589. [CrossRef]
41. Sing, K.S.W.; Everett, D.H.; Haul, R.A.W.; Moscou, L.; Pierotti, R.A.; Rouquerol, J.; Siemieniewska, T. Reporting Physisorption Data for Gas/Solid Systems with Special Reference to the Determination of Surface Area and Porosity. *Pure Appl. Chem.* **1985**, *57*, 603–619. [CrossRef]
42. Builes, S.; Vega, L.F. Understanding CO_2 Capture in Amine-Functionalized MCM-41 by Molecular Simulation. *J. Phys. Chem. C* **2012**, *116*, 3017–3024. [CrossRef]
43. Chanapattharapol, K.C.; Krachuamram, S.; Youngme, S. Study of CO_2 Adsorption on Iron Oxide Doped MCM-41. *Microporous Mesoporous Mater.* **2017**, *245*, 8–15. [CrossRef]
44. Silverstein, R.M.; Webster, F.X.; Kiemle, D.J.; Bryce, D.L. *Spectrometric Identification of Organic Compounds*, 7th ed.; John Wiley & Sons, Ltd.: Hoboken, NJ, USA, 2005; ISBN 0-471-39362-2.